

Review Article

MRI Contrast Agent-Based Multifunctional Materials: Diagnosis and Therapy

Hyeona Yim, Seogjin Seo, and Kun Na

Department of Biotechnology, The Catholic University of Korea, 43-1 Yeokkok2-dong, Wonmi-gu, Gyeonggi-do, Bucheon-si 420-743, Republic of Korea

Correspondence should be addressed to Kun Na, kna6997@catholic.ac.kr

Received 21 June 2011; Revised 17 August 2011; Accepted 17 August 2011

Academic Editor: Donglu Shi

Copyright © 2011 Hyeona Yim et al. This is an open access article distributed under the Creative Commons Attribution License, which permits unrestricted use, distribution, and reproduction in any medium, provided the original work is properly cited.

Various imaging technologies have become increasingly important in developing a better understanding of information on the biological and clinical phenomena associated with diseases of interest. Of these technologies, magnetic resonance imaging (MRI) is one of the most powerful for clinical diagnosis and in vivo imaging without the exposure to ionising radiation or radiotracers. Despite its many advantages, there are intrinsic limitations caused by MRI contrast agents, such as short vascular half-life circulation, which lead to unwanted side effects. In this review, we will focus on the multifunctional modification of MRI contrast agents for diagnosis and therapy.

1. Introduction

Powerful imaging tools such as fluorescence imaging (FI), magnetic resonance imaging (MRI), computed tomography (CT), positron emission tomography (PET), single-photon emission computed-tomography (SPECT), and ultrasound provide scientific and clinical information [1, 2]. The properties and characteristics of these imaging tools are summarised in Table 1. Among these technologies, MRI is one of the best noninvasive imaging modalities in both the clinical and basic research fields because of its ability to provide a wealth of spatial and temporal resolution. Moreover, it does not harm the patient because it uses strong magnetic fields and nonionising radiation in the radio frequency range, unlike CT and traditional X-rays, which both use ionising radiation. A basic understanding of MRI contrast is founded upon the nuclear magnetic resonance (NMR) phenomenon. MRI contrast is defined by the two-principle NMR processes of spin relaxation, T1 (longitudinal), and T2 (transverse) [3].

Based on MRI principles, several types of paramagnetic or superparamagnetic contrast agents have been used to enhance MRI contrast. MRI contrast agents work by shortening the T1 relaxation time of protons located nearby. The T1 shortening is due to an increase in the rate of stimulated

emission from high-energy states to low-energy states. Paramagnetic metal ions used as T1 contrast agents principally accelerate T1 relaxation and produce the “bright” contrast in a T1-weighted image, whereas superparamagnetic iron oxides (SPIOs) used as T2 contrast agents primarily increase the rate of T2 relaxation and create “dark” contrast effects. Although most paramagnetic (i.e., gadolinium (Gd)-based complexes) materials are currently employed in clinical applications, they must be modified for safety and functionality due to limitations caused by their very low molecule weights, which is many unwanted side effects [1, 4–6]. Additionally, the modification of SPIO particles by conjugating targeting moieties for their multifunctional modalities is required to overcome the particles’ limitations, such as their very short blood circulation time. However, their nanostructured agents are extensively used in the clinic or in research fields. This review surveys the development of nanostructured and multifunctional contrast agents for diagnosis and therapy in the MRI.

2. Nanostructured MRI Contrast Agents

The principal paramagnetic ions used as T1 contrast agents in MRI applications involve manganese (Mn), chromium

TABLE 1: Properties and characteristics of various imaging techniques.

| Modality | Probe | Spatial resolution | Advantages | Limit |
|------------------------------------|--|----------------------|--|--|
| Magnetic resonance imaging (MRI) | Paramagnetic metals (e.g., Gd and Mn) superparamagnetic metals (e.g., iron oxide) | 25–100 μm | High resolution no radiation physiological and anatomical details | In patient with limit (metallic devices) High cost |
| Optical imaging | Fluorescent dyes, quantum dots | 2–5 mm | High sensitivity functional information no radiation | Low resolution low tissue penetration |
| Computed tomography (CT) | Gold, iodine | 50–200 μm | High spatial resolution. differentiate between tissues. | Requires contrast agent Radiation tissue nonspecificity |
| Gamma scintigraphy (PET and SPECT) | Radionuclides (F-18, In-111, Cu-64) | 1–2 mm | Monitoring biochemical processes | Radiation low resolution high cost |

(Cr), and gadolinium (Gd). These metallic ions are relatively toxic in their free forms, but this toxicity may be reduced by chelation with ethylenediaminetetra acetic acid (EDTA), diethylenetriaminepenta acetic acid (DTPA), glucoheptonic acid, or desferrioxamine [7]. In particular, Gd chelates are currently available worldwide. Of the Gd chelate agents, gadopentetate dimeglumine (Gd-DTPA), gadoteridol, and gadodiamide (Gd-DTPA-BMA) have the greatest market share. These Gd chelate agents have been manufactured to be safe for the patient, and they follow strict FDA regulations to avoid any health complications. However, the low molecular weight Gd chelates are essentially first-pass agents, which may limit their use in other parts of the body. Most current commercial agents exhibit poor performance in several clinical applications, such as gastrointestinal tract and intravascular imaging, because of their systemic distribution despite their development [8].

These agents must be modified to target specific organs, regions of the body, or diseased tissue to gain the greatest diagnostic value from MRI. The requirements state that the agents must be designed to contain a large number of paramagnetic centres that can be selectively bound to the target tissue and that the modified agents must be of sufficiently high molecular weight to prolong vascular retention and, thus, slow tissue clearance. Over the past several years, there have been several approaches to produce structural modifications. These approaches include the conjugation of paramagnetic agents with macromolecular polymers, polymeric paramagnetic nanoparticles, and dendrimer-based metal chelates [9–11].

Kun Na developed Gd-DTPA chelate compounds by conjugation with pullulan (Gd-DTPA-pullulan, GDP) [5]. Pullulan, a natural and nonionic polysaccharide containing repeating maltotriose units condensed through α -1,6 linkage, has been reported to demonstrate a high affinity for asialoglycoprotein receptors in liver parenchymal cells, namely, hepatocytes [12]. Figure 1 Showed that GDP was able to distinguish between malignant and normal regions in delayed MRI. The signal intensities of GDP in regions of interest (ROI) were four times higher than those of Gd-DTPA-BMA. Additionally, GDP demonstrated a prolonged circulation time in the body compared to Gd-DTPA-BMA,

which resulted in enhanced discriminative contrast power of hepatocytes [5].

Cheng et al. reported that dendrimer nanoclusters (DNCs) are composed of individual Gd-labeled polyamidoamine (PAMAM) dendrimers that have been cross-linked to form larger nanoparticulate carriers. They also described how Gd-labeled DNCs could possibly target cancer tissues or cells specifically by conjugation with folic acid as a special ligand for ultrasensitive MRI detection of various cancer types of interest. As a consequence, the biodegradable dendrimer-based Gd-labeled nanoparticles exhibited longer circulation and retention times as compared to other Gd chelates and could be eliminated from the body within a reasonable period of time after performing their diagnostic function [13].

Additionally, Terreno's group reported the use of paramagnetic liposomes as contrast agents for monitoring the processes of drug delivery and release by MRI. Their formulation of liposome-loaded Gd chelates was proposed to allow the fast and full release of Gd chelates at pH 5.5 in endosomes using pH-sensitive liposomes. As a result, Gd-chelated contrast agents were released faster from pH-sensitive liposomes; this release was dependent on the reduction in pH. The image showed the highest intensity at pH 5.5 due to increased opportunity for contact with water molecules [14].

Unlike the widely used paramagnetic Gd chelates, the nanostructures of SPIOs composed of maghemite or magnetite crystals less than 20 nm in diameter contain thousands of Fe atoms and approach saturation magnetisation under a magnetic field typical. Each nanocrystal can generate signal contrast several orders of magnitude greater than a Gd chelate. Additionally, iron oxides have little known toxicity in in vivo applications. For these reasons, SPIOs have been researched extensively over the past two decades as a popular type of MRI contrast agent. However, general SPIOs have a short blood circulation half-life, especially in mice, which leads to their nonspecific uptake by cells in the blood, including macrophages. To increase the circulation and signal sensitivity of SPIOs for the in vivo imaging of molecular markers, their core must be coated with special functional moieties such as amphiphilic polymers or tumour-targeting ligands. SPIOs that circulate for longer may have an increased

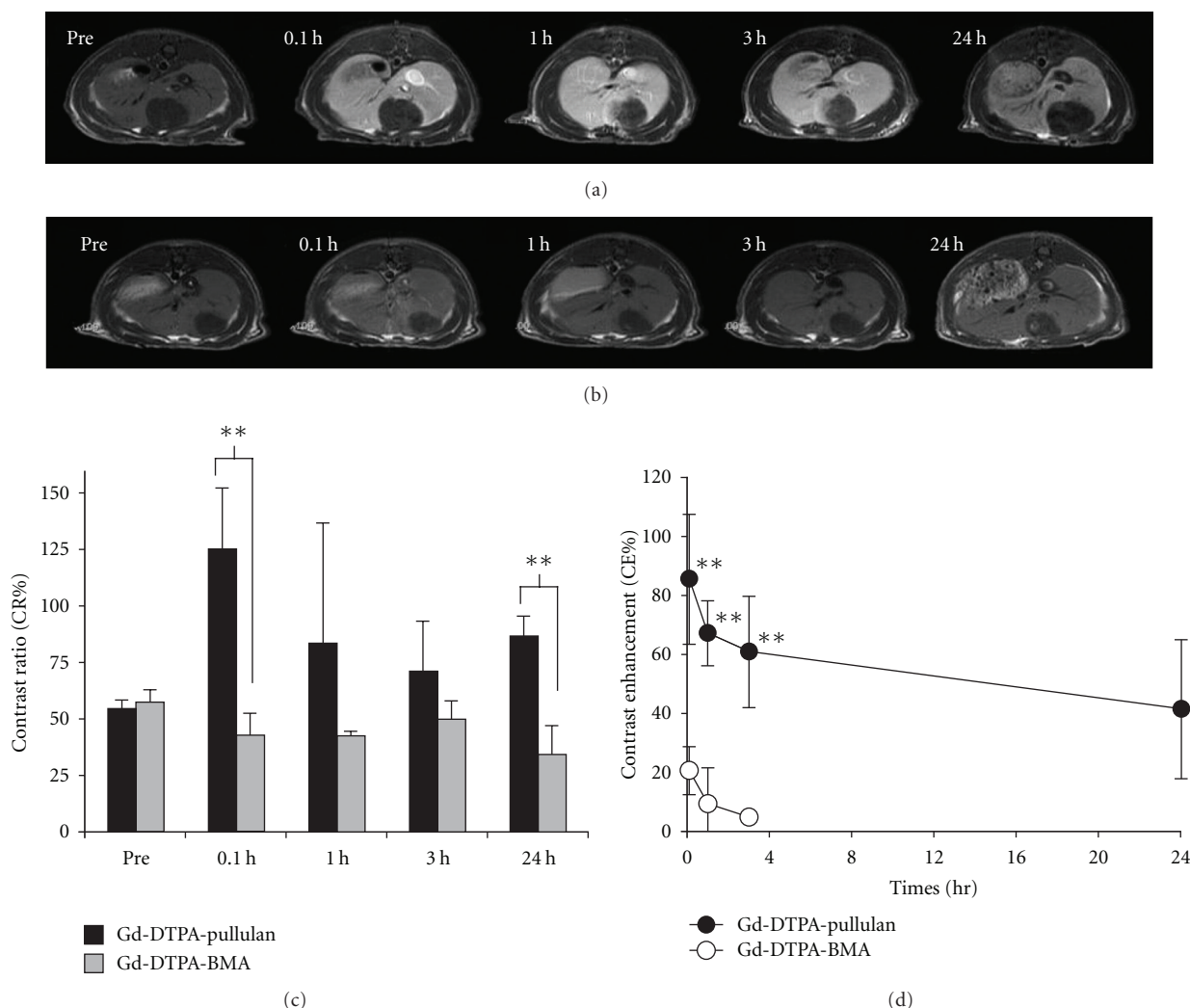


FIGURE 1: (a) and (b), time-dependent MR images of HCC rats after IV injection of Gd-DTPA-pullulan (a) and Gd-DTPA-BMA (b). (c), contrast ratio (CR) of Gd-DTPA-pullulan and Gd-DTPA-BMA; the CR is the relative contrast of hepatic lesion to normal region. (d), contrast enhancement (CE) of Gd-DTPA-pullulan and Gd-DTPA-BMA; the CE was calculated from the contrast ratio of the normal liver region between pre- and postinjection. Data are expressed as the mean \pm s.d ($n = 4$), (** $P < 0.01$, *** $P < 0.001$ with unpaired t -test) (see [5]).

chance of binding to the target molecules and thus produce enhanced contrast effect. However, most of the magnetic field surrounding coated SPIOs falls within the coating. Therefore, the coating molecules of SPIOs can expel water from their surface, hinder water diffusion, or immobilise nearby water molecules by forming hydrogen bonds; all these abilities may affect the nuclear relaxation of water protons. To prevent this interference, a dual solvent-exchange method has been employed to coat nanocrystals with small amphiphilic molecules, such as poloxamer and hydrophobically modified PEG [15, 16].

Tong et al. focused on a versatile coating method to generate an array of water-soluble SPIOs with different core sizes and coating thicknesses for signal enhancement. Using a dual solvent-exchange method, iron oxide cores were coated with a 1,2-distearoyl-sn-glycero-3-phosphoethanolamine-N-[methoxy (polyethylene glycol)] copolymer (DSPE-mPEG)

in which amphiphilic DSPE-mPEG on the hydrophobic surface of a nanocrystal can be induced by enhancing the polarity of solvent systems, which results in increased water solubility of SPIOs (Figure 2). The resulting DSPE-mPEG coating is stable and versatile and offers an optimal shell/core ratio. DSPE-mPEG-coated SPIO nanocrystals can increase the intensity of iron oxide under the optimal conditions by controlling the size and thickness of iron oxide [16].

Chertok et al. also reported the use of PEGylated silane-coated magnetic iron oxide nanoparticles to enhance MRI contrast in tumours. After intravenous injection, greater accumulation of colloidal stable PEGylated magnetic nanoparticles in the 40 nm size range was observed in murine tumours as compared to those in the 20 nm size range [17].

In addition to size control, surface modification by conjugation with specific ligands is of critical importance in

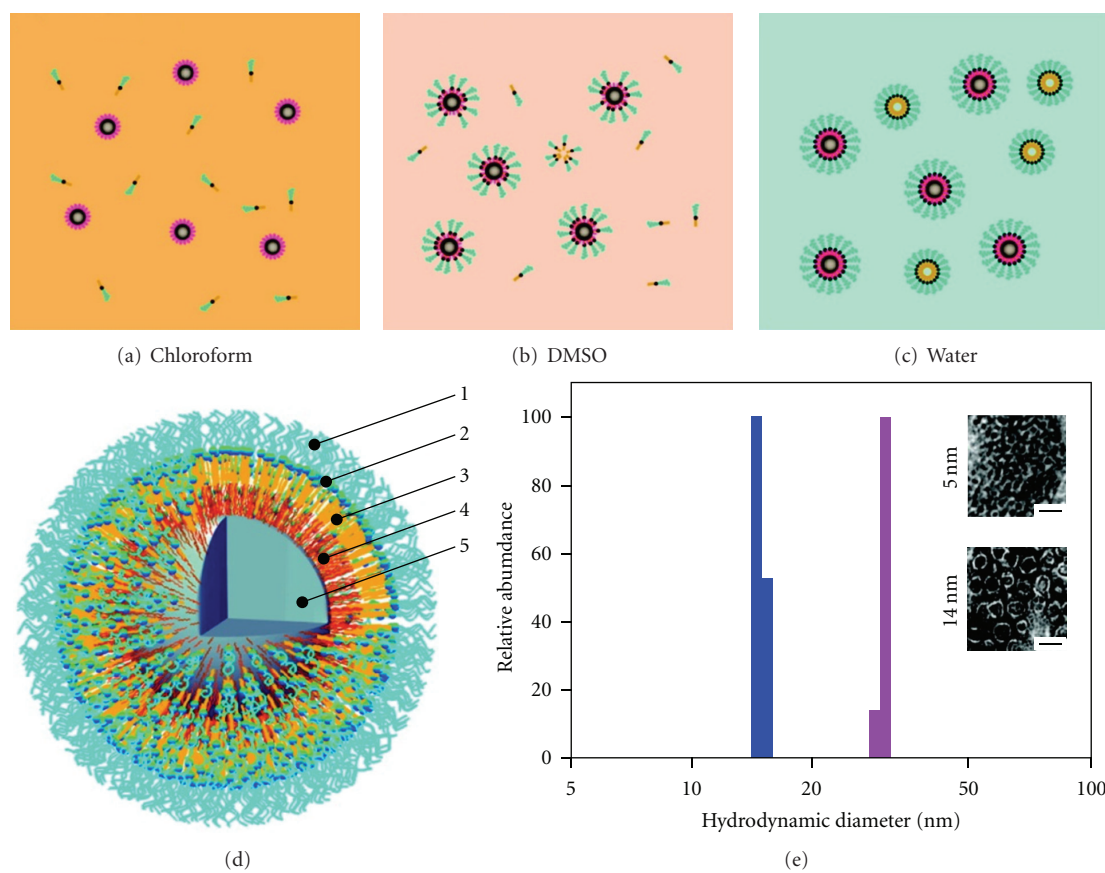


FIGURE 2: Schematic diagram of the SPIO synthesis and coating. (a) Both iron oxide cores and DSPE-PEG are dissolved in chloroform. (b) The addition of DMSO induces assembly between iron oxide cores and DSPE-PEG molecules. (c) The transition into water further strengthens the hydrophobic interaction between DSPE-PEG and oleic acid/oleylamine on the iron oxide cores. Due to its extremely low critical micelle concentration ($\sim 5 \mu\text{M}$ in water), unoccupied DSPE-PEG exists mainly in the form of empty micelles. (d) A schematic diagram of a SPIO with a 4.8-nm iron oxide core and DSPE-mPEG1000 coating. Layers 1 through 5 represent PEG, phosphate, DSPE, oleic acid/oleylamine, and the iron oxide core, respectively. The dimensions are based on transmission electron microscopy (TEM) measurements and numerical analysis (supporting information, SII and SIII). (e) Dynamic light scattering of the SPIOs coated with DSPE-mPEG1000: blue, number-weighted size distribution of 5 nm iron oxide core coated with DSPE-mPEG1000, average size 14.8 (1.2 nm); purple, 14 nm iron oxide core coated with DSPE-mPEG1000, average size 28.6 (0.4 nm). Shown in the inset are TEM images of coated SPIOs negatively stained with phosphotungstic acid to yield a white layer surrounding the iron oxide cores that indicate the DSPE-mPEG1000 coating layer (see [16]).

determining the pharmacokinetic profile of the iron oxide nanoparticles and the success of in vivo targeting. Among the neoplastic markers, integrin $\alpha_v\beta_3$, a cell adhesion molecule, plays a vital role in tumour angiogenesis and metastasis. Arginine-glycine-aspartic acid (RGD) peptide sequences are well known as specific probes for integrin targeting. RGD-iron oxide nanoparticle conjugates have been developed for integrin targeting. Chen's group reported the use of iron oxide nanoparticles-RGD conjugates coated with a PEGylated amphiphilic triblock copolymer composed of segments of polybutylacrylate, polyethylacrylate, polymethacrylic acid, octylamine, and a hydrophobic hydrocarbon side chain for tumour integrin targeting and MRI. A triblock copolymer was subsequently coated onto the particle surface, which resulted in a bilayer coating with multiple amine-terminated PEG chains exposed outside. Thus, a triblock copolymer renders the iron oxide-RGD nanoparticles water soluble.

Such a phase transfer is straightforward with high throughput and high yield. Clear tumour contrast was observed by MRI with RGD-triblock PEGylated iron oxide nanoparticles, indicating successful RGD-integrin governed tumour targeting and remarkably limited hepatic uptake [18]. PEGylated iron oxide-RGD conjugates showed excellent tumour integrin binding efficiency and specificity as well as limited reticuloendothelial system (RES) uptake for molecular MRI. In summary, size control and functional surface modification easily increases the intensity and efficacy of the contrast agent for diagnosis.

The gadolinium hybrid nanoparticulate MRI contrast agents also have been reported as gadolinium oxide [19], gadolinium fluoride [20], and gadolinium phosphate [21], are different from gadolinium chelate compound. Gadolinium hybrid MRI contrast agents, which were composed of a gadolinium oxide core, show a higher signal-to-noise ratio

and a better anatomic resolution in T1-weighted images due to having nanoparticulate shapes, lower r_2/r_1 values. These nanoparticles were dispersed in aqueous phase [21].

Olivier Tillement group have been offered contrast agent, which gadolinium oxide core embedded in a polysiloxane shell. This contrast agent is functionalized by organic dyes at inner phase and shielded by PEG at outer phase and is well appropriated in vivo dual modality magnetic resonance and fluorescence imaging. The hydrodynamic diameter is 8.9 nm, and core size is 4.6 nm. These hybrid gadoliniums are able to circulate in the vessels without aggregation since no uptake was observed in the liver, and the particles were naturally eliminated by renal excretion due to small size [22].

GdF₃ nanoparticles were conjugated with 2-aminoethyl phosphate group (GdF₃/LaF₃: AEP) or citrate group (GdF₃: cit) [20]. The surface of gadolinium nanoparticles has been shown positive or negative charge by outer group. Dextran-coated GdPO₄ nanoparticles (PGP/dextran-K01) were synthesized by a hydrothermal process in the presence of dextran [21]. The advantage of these gadolinium hybrid nanoparticulate MRI contrast agents is higher solubility, higher relaxivity than chelated gadolinium at identical gadolinium concentration [23].

3. Multimodal MRI Contrast Agent: Fluorescence, CT, and PET

Multimodal contrast agents can provide more accurate and detailed information associated with diseases than single contrast agents. MRI is able to achieve deep penetration of light into tissues and provide anatomical details and high quality 3D images of soft tissue [6, 24] but exhibits lower sensitivity than radioactive or optical methods. In contrast, FI has much higher sensitivity and potential for real-time imaging, but it has limited depth perception [25]. As a consequence, intensive attempts have been made to develop MRI-FI nanoprobe due to their prominent advantages for medical diagnosis.

Hoshino et al. reported a simple and versatile method to develop dual modality nanoprobe by incorporating paramagnetic Gd ions onto surface modified-quantum dots (QDs) with zinc oxide nanocrystals. Surface modification of QDs is essential to prevent self-aggregation and loss of luminescence in the intracellular environment or under isotonic conditions. However, these molecules are excellent candidates for organic fluorophores based on their high luminescence, stability against photobleaching, and a range of fluorescence wavelengths from blue to infrared depending on particle size [26]. The typical transmission electron microscopy (TEM) images in Figures 3(a) and 3(b) depicted the diameters of ZnO QDs and Gd-doped ZnO QDs ($x = 0.08$) as approximately 6 nm and 4 nm, respectively. Nevertheless, in the sample with a higher Gd concentration ($x = 0.3$), the particles were so small that they could not be seen clearly (Figure 3(c)). Meanwhile, selected area electron diffraction analysis presented similar patterns for ZnO QDs and Gd-doped ZnO QDs ($x = 0.08$ and 0.3), and all the diffraction rings could be indexed to wurtzite ZnO. The high resolution

TEM images shown in Figures 3(d) and 3(e) revealed lattice fringes with a spacing of approximately 0.26 nm for both ZnO QDs and Gd-doped ZnO QDs ($x = 0.08$), which was very consistent with the lattice spacing in the (0.02) planes of the ZnO wurtzite phase. This result suggests that Gd doping did not induce any significant lattice distortions of ZnO QDs. However, when x increased to 0.3, the crystallinity of the ZnO QDs became so weak that no clear lattice fringe could be observed (Figure 3(f)). These properties of Gd-doped ZnO QDs are allowed to function as effective dual modal imaging nanoprobe due to their effect on the T1 relaxation time, and they remain high viability even at a high dose of QDs [25]. Although many efforts have been made to reduce the intrinsic toxicity and maintain the long-term photostability of QDs by conjugation with paramagnetic agents or in combination with dye-doped silica and SPIOs as multimodal imaging probes, the size control problem remained an issue because their fluorescence sensitivity depends on particle size. To solve the problem, the Hyeon group reported the combination of QDs and upconverting nanoparticles (UCNPs) such as NaYF₄:Yb³⁺, Er³⁺ and NaYF₄:Yb³⁺, Tm³⁺ to yield bimodal imaging probes that can provide the high sensitivity and resolution of fluorescence imaging as well as the noninvasive and real-time monitoring abilities of MRI. As UCNPs absorb near-infrared (NIR) photons and emit visible or near-UV photons, optical imaging with these nanoparticles has several advantages over conventional fluorescence imaging: (1) the signal-to-noise ratio and detection sensitivity are improved because autofluorescence is absent; (2) in vivo imaging is facilitated by deep penetration of noninvasive NIR excitation; (3) photodamage to living organisms is very low. Unlike other nanocomposites that exhibit multimodality, UCNPs work alone and do not require the addition of any other moieties. The deep penetration depth of NIR excitation, excellent photostability, and absence of autofluorescence of UCNPs make them suitable for applications such as targeting of tumour tissues in vivo and long-term cellular and/or animal imaging [27].

The X-ray, CT imaging widely used for diagnosis, generates accurate and bright images. However, it is necessary to administer a contrast agent. These agents include iodinated molecules [28, 29] that have rapid pharmacokinetics and high viscosity, which most likely leads to allergic reaction. Many alternatives to iodinated contrast have recently been developed to overcome these intrinsic problems. Gold-encapsulated Gd chelate nanoparticles are considered alternative contrast agents for medical imaging because the properties of gold nanoparticles include a relatively longer vascular half-life than other molecular contrast agents. Taken together, gold nanoparticles combined with fluorescence imaging and MRI are probably the most frequently studied because they join the high sensitivity of the fluorescence phenomenon with the increased spatial resolution of MRI. Alric's group reported that the gold-encapsulated Gd chelates, which have a multilayered organic shell, bound to each other through disulphide bonds for both X-ray, CT and MRI. The contrast enhancement in the MRI resulted from the presence of Gd ions trapped in the organic shell, whereas

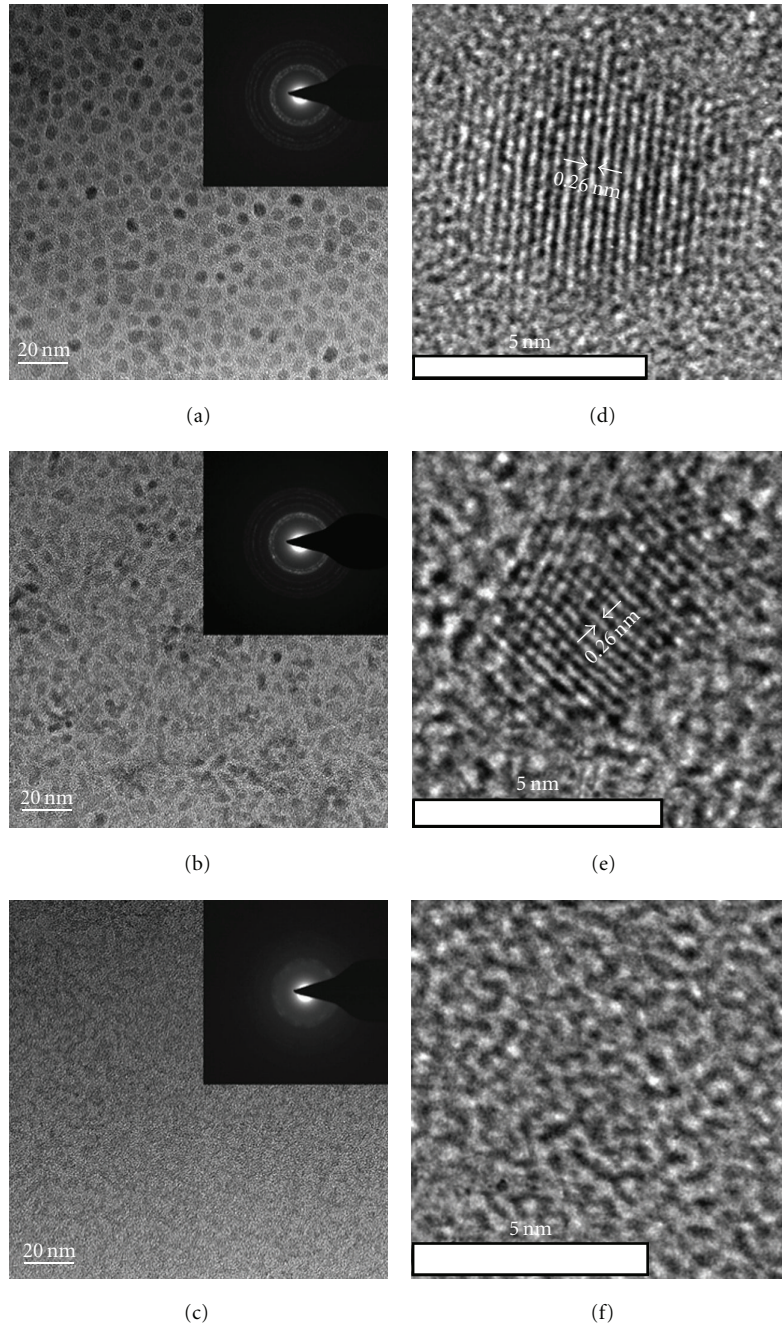


FIGURE 3: (a)–(c) TEM images of Gd-doped ZnO QDs with $x = 0, 0.08$ and 0.3 . The insets show the corresponding electron diffraction patterns. (d)–(f) High-resolution TEM images of Gd-doped ZnO QDs with $x = 0, 0.08$ and 0.3 (see [48]).

the gold core provided strong X-ray absorption. The results revealed that the Gd-bound gold nanoparticles used for dual modality imaging freely circulate in the blood vessels without undesirable uptake by macrophages [30].

PET is an analytical imaging tool that uses signals emitted by compounds labelled with positron-emitting radioisotopes such as fluorine-18 as molecular probes to image and measures biochemical processes of mammalian biology in vivo. Advances in PET using established imaging tools have resulted in spatial resolution greater than 2 mm [31, 32].

However, it may still be impossible to accurately localize an area of increased activity using PET images alone due to the absence of identifiable anatomical structures, particularly in the abdomen. Although a simultaneous PET/CT scanner that precisely and simultaneously registers functional data from PET and anatomical image from CT is used to solve the limitations on a routine basis in clinical oncology, the intrinsic functional resolution restrictions of PET and PET/CT remain the same. In addition to accurate functional and anatomical localization, highly accurate image registration, which can be

provided by MRI, is required to correct PET partial volume effects and aid in PET image reconstruction. Compared with PET/CT, PET/MRI has the advantage of greatly reducing radiation exposure. Polyaspartic acid-coated iron oxide nanoparticles conjugated with cyclic RGD peptides and the macrocyclic chelating agent 1,4,7,10-tetraazacyclododecane-N,N',N'',N''',-tetraacetic acid (DOTA) for integrin $\alpha_v\beta_3$ recognition and positron-emitting radionuclide ^{64}Cu (half-life [$t_{1/2}$] = 12.7 h) labelling were prepared for dual PET/MRI of tumour integrin $\alpha_v\beta_3$ expression in vivo. This bifunctional imaging approach to PET/MRI may allow for earlier tumour detection with a high degree of accuracy and provide further insight into the molecular mechanisms of cancer [33].

Jeongsoo Yoo and his coworkers developed magnetism-engineered iron oxide (MEIO) with a composition of MnFe_2O_3 (MnMEIO), which has exceptionally high MRI contrast effects. They also prepared serum albumin (SA)-coated MnMEIO nanoparticles conjugated with ^{124}I ($t_{1/2}$ = 4.2 days, β^+ 23%) (^{124}I -SA-MnMEIO) as molecular nanoprobe for dual modality PET/MRI because the T2 relaxivity coefficient is two or three times better than that of conventional iron oxide-based SPIO probes (Figure 4). The accurate positioning of brachial lymph nodes (LN) was achieved when PET and MRI were overlaid. Two different types of LNs could be clearly identified and accurately localized in a PET/MR fusion image as a result of the highly complementary nature of the PET and MRI techniques [34].

Recently, PET/MRI/near-infrared fluorescence (NIRF) trimodality imaging contrast agents have been researched to gain precise information about diseases [35]. For example, serum albumin(SA)-coated iron oxide nanoparticles dually labelled with ^{64}Cu -DOTA and Cy5.5 were tested in a subcutaneous U87MG xenograft mouse model. With the compact SA coating, the nanoparticles demonstrated a prolonged circulation half-life, and they also showed massive accumulation in lesions, a high extravasation rate, and low uptake of the nanoparticles by macrophages at the tumour area. The MRI contrast agents combined with other techniques have been developed to increase the sensitivity around the disease region. Furthermore, with instrument development of the diagnostic hardware, advances in nanoparticle-based probes are a prerequisite for successful multimodal diagnosis.

4. Multifunctional MRI Contrast Agent: Drug Delivery and Cell Tracking

Multifunctional MRI contrast agents loaded with drugs have received considerable attention as attractive carriers for diagnosis and therapy.

The magnetic nanoparticle can serve as both a contrast agent for MRI and a drug carrier for delivery. Nanoparticles have been designed to possess specific properties, including highly accurate targeting to specific regions containing the cell types of interest [36–38]. For example, after anticancer drug-loaded SPIO nanoparticles conjugated with specific ligands are injected into an intravenous vessel, the nanoparticles can easily reach the tumour area by systemic delivery

with specific ligands and simultaneously release the anticancer drugs at the tumour sites. Additionally, the process can be monitored in real time by MRI contrast agents.

The pH-triggered system is currently one of the most extensively studied stimulus systems for cancer therapy because the increased aerobic glycolysis, or the Warburg effect, in cancer cells leads to the lower extracellular pH of cancer cells (pH 6.5 to 7.2). Based on this system, anti-HER2/neu (HER: herceptin) antibody-modified pH-sensitive drug-delivering magnetic nanoparticles (HER-DMNP) were investigated as a prototype of theragnosis for effective cancer therapy guided by molecular imaging [39]. The nanoparticles are delivered to herceptin and release the anticancer drug (i.e., doxorubicin, DOX) because of the low extracellular pH (Figure 5). Simultaneously, the magnetic nanoparticles serve as MRI contrast agents to show a vivid contrast image [40].

Additionally, the magnetic particles can be designed for hyperthermia in cancer treatment in the magnetic field and degraded into nontoxic iron ions in vivo [41–43]. Thermally cross-linked SPIO nanoparticles (TCL-SPIONs) coated with protein- or cell-resistant polymers serve as MRI contrast agents and induce the anticancer effect in the magnetic field. TCL-SPIONs reduced the side effects when compared to free DOX because of the excellent cancer targeting efficiency created by the enhanced permeability and retention (EPR) effect. The antibiofouling polymer-coated TCL-SPIONs can circulate long term in the vascular system by escaping from uptake by RES. After administering the coated TCL-SPIONs into tumour xenograft mice by intravenous injection, the tumour could be detected by T2-weighted MRI within 1 h as a result of the accumulation of nanomagnets within the tumour site. Consequently, TCL-SPIONs have been developed as multifunctional smart agents for theragnosis [42, 44, 45].

A nanostructured multifunctional smart MRI contrast agent is also suitable and effective as a drug carrier for a variety of chemotherapeutic agents [46, 47].

The visualisation of transplanted stem cells with a noninvasive technique is essential for cell implantation. MRI may be the best technique for cell tracking based on its high spatial and temporal resolution and free selection of the imaging plane. For MRI observation, stem cells must be marked by magnetic labelling to distinguish them from existing cells in the organ. Despite several trials of modifications of SPIONs via linking to peptides or monoclonal antibodies, the results lead to some potential problems, technical complexity, and poor availability in cell labelling procedures. Liu et al. reported the development of low-molecular-weight polyethylenimine (PEI)/SPIO nanocomposites with efficient cell-labelling capability. PEI-wrapped magnetic nanoparticles easily interacted with cell membranes of stem cells and were monitored with a clinical 3T MRI system [48] (Figure 6).

Gd-based contrast agents are also suitable for the monitoring and fate mapping of stem cells in a T1-weighted image. Dong-Ming Huang's group studied the use of dual functional mesoporous silica nanoparticles (MSNs) conjugated with fluorescent isothiocyanate and Gd chelates (Gd-Dye MSNs) for stem cell tracking and high contrast efficacy. Stem cells

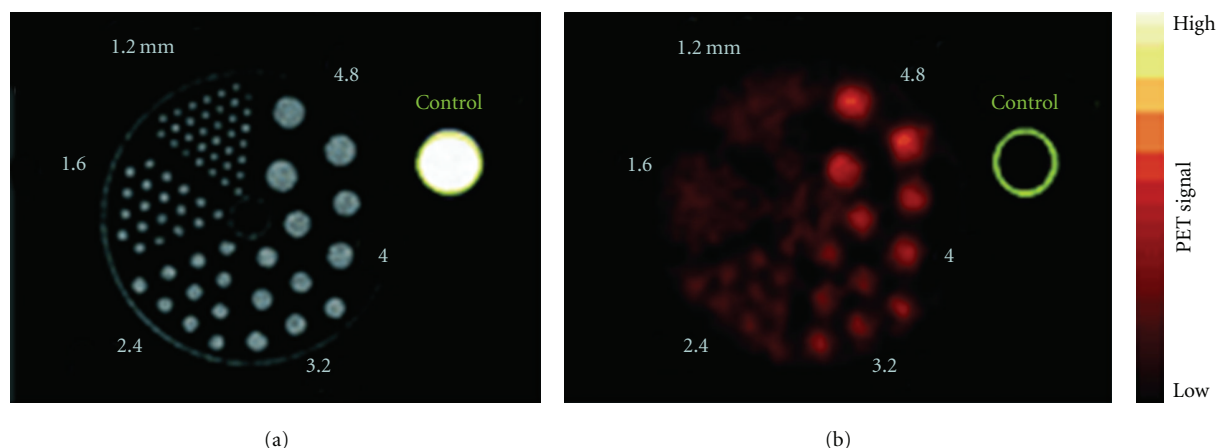


FIGURE 4: Comparison of spatial resolution of (a) MRI and (b) PET techniques with a Derenzo phantom (circle diameters of 1.2, 1.6, 2.4, 3.2, 4.0, and 4.8 mm), which contains the contrast agents MnMEIO ($50 \mu\text{g mL}^{-1}$ (Mn+Fe)) and ^{124}I ($2.5 \mu\text{Ci mL}^{-1}$); yellow circle: water (control). MnMEIO: Mn-doped magnetism-engineered iron oxide (see [34]).

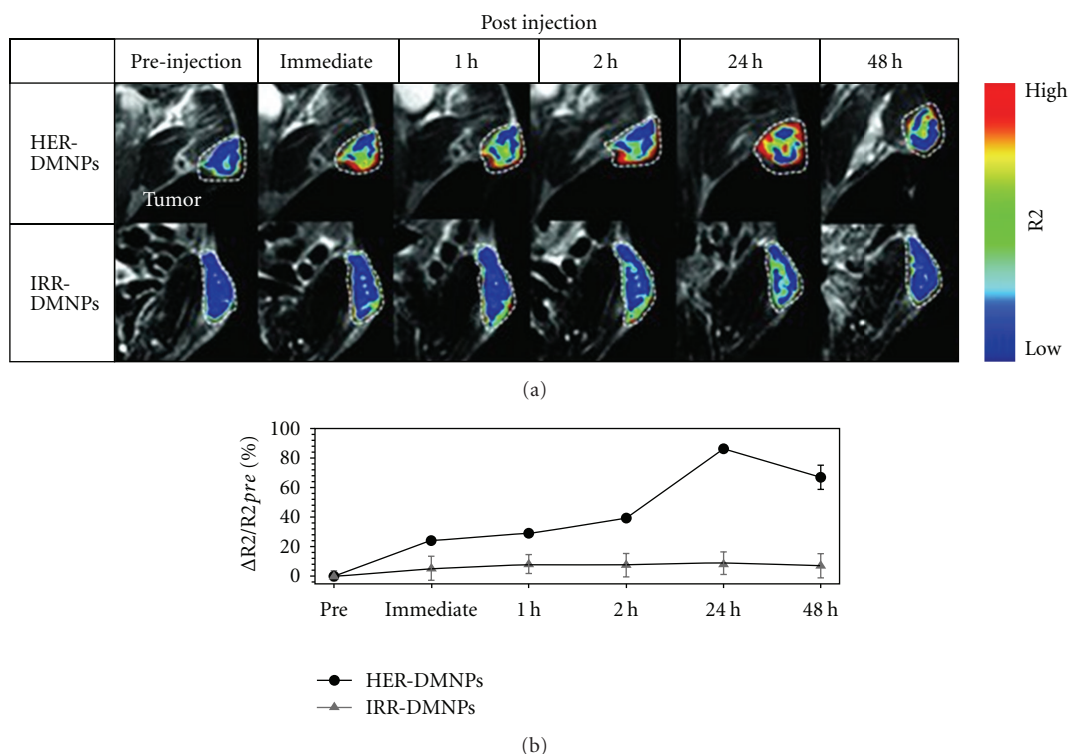


FIGURE 5: (a) Color-coded T2-weighted MR images of tumor-bearing mice after the intravenous injection of HER-DMNPs and IRR-DMNPs at various time intervals, respectively. Tumor regions are indicated with a white dashed boundary. (b) $\Delta R2/R2_{pre}$ graph versus time after the injection of HER-DMNPs (black circle) and IRR-DMNPs (gray triangle) (see [40]).

labelled with Gd-Dye MSNs in an endocytosis-mediated manner were detected with a 1.5T MRI for at least 14 days. Gd-Dye MSNs did not affect cytotoxicity, growth, or differentiation of hMSCs [49].

Song et al. described Gd-enriched polyvalent DNA-gold nanoparticle conjugates (DNA-AuNPs) with the ability to efficiently penetrate cells and accumulate to a level that provides sufficient contrast enhancement for the imaging of

small cell populations with micro-sized Gd incubation concentrations. Moreover, labelling of the conjugates with a fluorescent dye permitted multimodal imaging to confirm cellular uptake and intracellular accumulation and provide a means for histological validation. These particles exhibit a high loading efficiency of Gd, a 50-fold increase in cellular uptake compared to the commercial Gd-DOTA, and relatively high relaxivity [50].

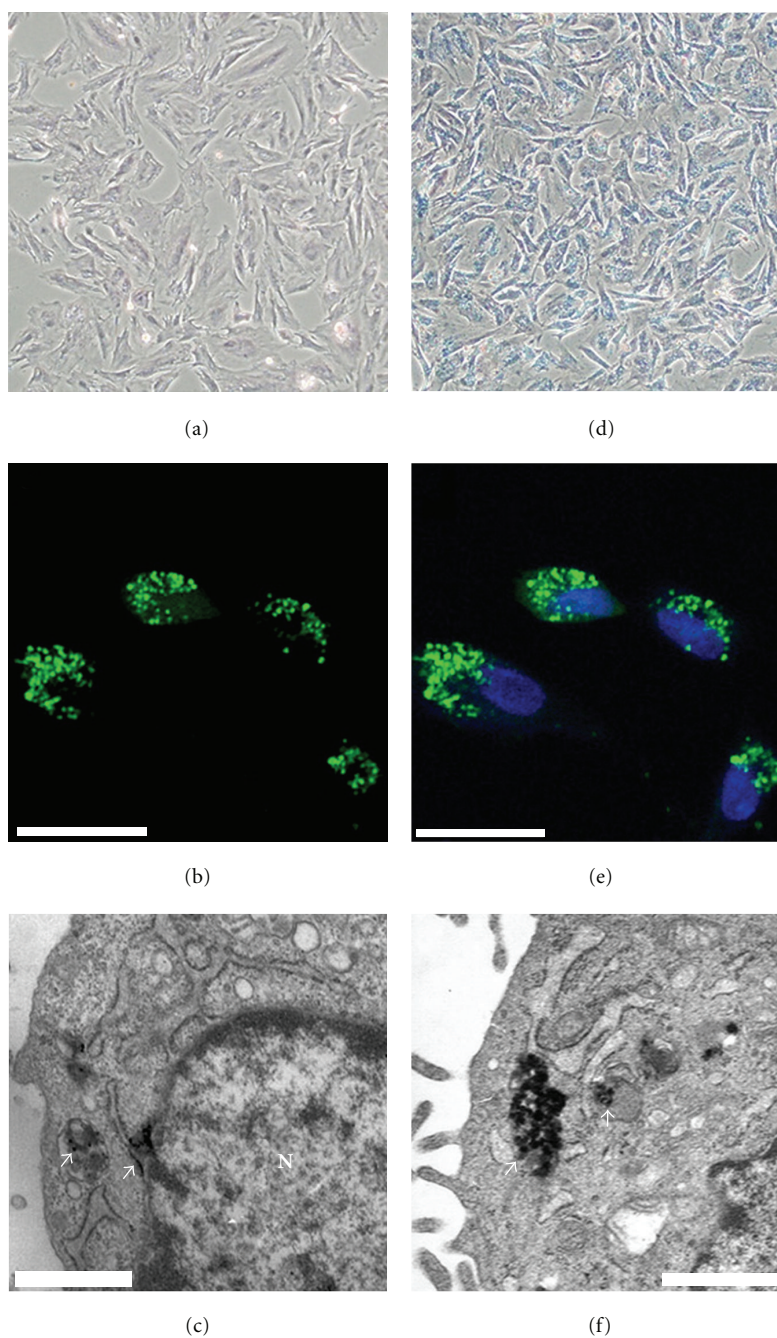


FIGURE 6: Mesenchymal stem cells (MSCs) labeled with alkyl-PEI/SPIO nanocomposites. Prussian blue staining of unlabeled MSCs (a) and SPIO-labeled MSCs (b) (7 mg Fe/mL, 24 h). The morphology of these SPIO-labelled MSCs is not changed, and blue granules were evident in the cytoplasm around the nuclei; CLSM investigation of the SPIO-labeled MSCs before (c) and after merging with nuclei (d). Electron microscopy of cells labelled with SPIO probes (arrows) (e, f). Magnification (a, b), scale bar 1/4 10 mm (c, d), scale bar 1/4 50 nm (e), scale bar 1/4 100 nm (f) (see [48]).

5. Conclusion

Functionally modified MRI contrast agents with enhanced intensity and sensitivity may improve diagnostic technique as well as therapeutic efficacy. Additionally, the use of multi-modal contrast agents with other types of imaging tools can maximize their prominent advantages and compensate for

their intrinsic disadvantages to provide excellent diagnostic images with anatomical and functional information.

Also, the safety of contrast agent should be considered to overcome its limit of use in clinic. In previous study, contrast agent does not cause side effects in normal patients whereas generates serious nephrogenic system fibrosis (NSF) in patient with failure kidney. NFS is emerging systemic

disordered character by widespread tissue fibrosis [5]. The body clearance ways and distribution of MRI contrast agent is one to the very important topic in use of contrast agent to reduce the side effect. For this reason, contrast agent should be designed to be able to perfectly remove from body through kidney and bile without accumulation in body and not separated into free gadolinium from chelated compounds.

The development of contrast agents has been accelerated with advance of several nanotechnologies over the past decade. Contrast agents that use new nanotechnology must continue to increase their theranostic efficiency and safety in clinical and research applications.

Acknowledgments

This research was financially supported by the Fundamental R&D Program for Core Technology of Materials, Republic of Korea, the Gyeonggi Regional Research Center (GRRC), the Ministry of Knowledge Economy (MKE), and the Korea Industrial Technology Foundation (KOTEF) through the Human Resource Training Project for Strategic Technology, Republic of Korea.

References

- [1] J. Kim, Y. Piao, and T. Hyeon, "Multifunctional nanostructured materials for multimodal imaging, and simultaneous imaging and therapy," *Chemical Society Reviews*, vol. 38, no. 2, pp. 372–390, 2009.
- [2] L. Frullano and T. J. Meade, "Multimodal MRI contrast agents," *Journal of Biological Inorganic Chemistry*, vol. 12, no. 7, pp. 939–949, 2007.
- [3] G. M. Lanza, P. M. Winter, S. D. Caruthers et al., "Magnetic resonance molecular imaging with nanoparticles," *Journal of Nuclear Cardiology*, vol. 11, no. 6, pp. 733–743, 2004.
- [4] M. A. Hahn, A. K. Singh, P. Sharma, S. C. Brown, and B. M. Moudgil, "Nanoparticles as contrast agents for in-vivo bioimaging: current status and future perspectives," *Analytical and Bioanalytical Chemistry*, vol. 399, no. 1, pp. 3–27, 2011.
- [5] H. Yim, S.-G. Yang, Y. S. Jeon et al., "The performance of gadolinium diethylene triamine pentaacetate-pullulan hepatocyte-specific T1 contrast agent for MRI," *Biomaterials*, vol. 32, no. 22, pp. 5187–5194, 2011.
- [6] C. Sun, J. S. H. Lee, and M. Zhang, "Magnetic nanoparticles in MR imaging and drug delivery," *Advanced Drug Delivery Reviews*, vol. 60, no. 11, pp. 1252–1265, 2008.
- [7] D. H. Carr, J. Brown, and G. M. Bydder, "Gadolinium-DTPA as a contrast agent in MRI: initial clinical experience in 20 patients," *American Journal of Roentgenology*, vol. 143, no. 2, pp. 215–224, 1984.
- [8] C. H. Reynolds, N. Annan, K. Beshah et al., "Gadolinium-loaded nanoparticles: new contrast agents for magnetic resonance imaging," *Journal of the American Chemical Society*, vol. 122, no. 37, pp. 8940–8945, 2000.
- [9] X. Montet, K. Montet-Abou, F. Reynolds, R. Weissleder, and L. Josephson, "Nanoparticle imaging of integrins on tumor cells," *Neoplasia*, vol. 8, no. 3, pp. 214–222, 2006.
- [10] C. J. Sunderland, M. Steiert, J. E. Talmadge, A. M. Derfus, and S. E. Barry, "Targeted nanoparticles for detecting and treating cancer," *Drug Development Research*, vol. 67, no. 1, pp. 70–93, 2006.
- [11] C. Zhang, M. Jugold, E. C. Woenne et al., "Specific targeting of tumor angiogenesis by RGD-conjugated ultrasmall superparamagnetic iron oxide particles using a clinical 1.5-T magnetic resonance scanner," *Cancer Research*, vol. 67, no. 4, pp. 1555–1562, 2007.
- [12] M. R. Rekha and C. P. Sharma, "Pullulan as a promising biomaterial for biomedical applications: a perspective," *Trends in Biomaterials and Artificial Organs*, vol. 20, no. 2, pp. 111–116, 2007.
- [13] Z. Cheng, D. L. J. Thorek, and A. Tsourkas, "Gadolinium-conjugated dendrimer nanoclusters as a tumor-targeted T1 magnetic resonance imaging contrast agent," *Angewandte Chemie - International Edition*, vol. 49, no. 2, pp. 346–350, 2010.
- [14] E. Torres, F. Mainini, R. Napolitano et al., "Improved paramagnetic liposomes for MRI visualization of pH triggered release," *Journal of Controlled Release*, vol. 154, no. 2, pp. 196–202, 2011.
- [15] S. S. Yu, R. L. Scherer, R. A. Ortega et al., "Enzymatic- and temperature-sensitive controlled release of ultrasmall superparamagnetic iron oxides (USPIOs)," *Journal of Nanobiotechnology*, vol. 9, article 7, 2011.
- [16] S. Tong, S. Hou, Z. Zheng, J. Zhou, and G. Bao, "Coating optimization of superparamagnetic iron oxide nanoparticles for high T2 relaxivity," *Nano Letters*, vol. 10, no. 11, pp. 4607–4613, 2010.
- [17] B. Chertok, A. E. David, and V. C. Yang, "Polyethyleneimine-modified iron oxide nanoparticles for brain tumor drug delivery using magnetic targeting and intra-carotid administration," *Biomaterials*, vol. 31, no. 24, pp. 6317–6324, 2010.
- [18] K. Chen, J. Xie, H. Xu et al., "Triblock copolymer coated iron oxide nanoparticle conjugate for tumor integrin targeting," *Biomaterials*, vol. 30, no. 36, pp. 6912–6919, 2009.
- [19] M. A. McDonald and K. L. Watkin, "Investigations into the physicochemical properties of dextran small particulate gadolinium oxide nanoparticles," *Academic Radiology*, vol. 13, no. 4, pp. 421–427, 2006.
- [20] F. Evanics, P. R. Diamente, F. C. J. M. Van Veggel, G. J. Stanisz, and R. S. Prosser, "Water-soluble GdF3 and GdF3/LaF3 nanoparticles—physical characterization and NMR relaxation properties," *Chemistry of Materials*, vol. 18, no. 10, pp. 2499–2505, 2006.
- [21] H. Hifumi, S. Yamaoka, A. Tanimoto, D. Citterio, and K. Suzuki, "Gadolinium-based hybrid nanoparticles as a positive MR contrast agent," *Journal of the American Chemical Society*, vol. 128, no. 47, pp. 15090–15091, 2006.
- [22] J. L. Bridot, A. C. Faure, S. Laurent et al., "Hybrid gadolinium oxide nanoparticles: multimodal contrast agents for in vivo imaging," *Journal of the American Chemical Society*, vol. 129, no. 16, pp. 5076–5084, 2007.
- [23] J. L. Bridot, D. Dayde, C. Rivière et al., "Hybrid gadolinium oxide nanoparticles combining imaging and therapy," *Journal of Materials Chemistry*, vol. 19, no. 16, pp. 2328–2335, 2009.
- [24] C. F. G. C. Geraldes and S. Laurent, "Classification and basic properties of contrast agents for magnetic resonance imaging," *Contrast Media and Molecular Imaging*, vol. 4, no. 1, pp. 1–23, 2009.
- [25] Y. Liu, K. Ai, Q. Yuan, and L. Lu, "Fluorescence-enhanced gadolinium-doped zinc oxide quantum dots for magnetic resonance and fluorescence imaging," *Biomaterials*, vol. 32, no. 4, pp. 1185–1192, 2011.
- [26] A. Hoshino, K. Fujioka, T. Oku et al., "Physicochemical properties and cellular toxicity of nanocrystal quantum dots

- depend on their surface modification,” *Nano Letters*, vol. 4, no. 11, pp. 2163–2169, 2004.
- [27] Y. I. Park, J. H. Kim, K. T. Lee et al., “Nonblinking and nonbleaching upconverting nanoparticles as an optical imaging nanoprobe and T1 magnetic resonance imaging contrast agent,” *Advanced Materials*, vol. 21, no. 44, pp. 4467–4471, 2009.
- [28] J. M. Idee, I. Nachman, M. Port et al., “Iodinated contrast media: from non-specific to blood-pool agents,” in *Contrast Agents II*, pp. 151–171, Springer, Berlin, Germany, 2002.
- [29] W. Krause and P. Schneider, “Chemistry of X-ray contrast agents,” in *Contrast Agents II*, pp. 107–150, Springer, Berlin, Germany, 2002.
- [30] C. Alric, J. Taleb, G. Le Duc et al., “Gadolinium chelate coated gold nanoparticles as contrast agents for both X-ray computed tomography and magnetic resonance imaging,” *Journal of the American Chemical Society*, vol. 130, no. 18, pp. 5908–5915, 2008.
- [31] S. S. Gambhir, “Molecular imaging of cancer with positron emission tomography,” *Nature Reviews Cancer*, vol. 2, no. 9, pp. 683–693, 2002.
- [32] W. A. Weber, “Use of PET for monitoring cancer therapy and for predicting outcome,” *Journal of Nuclear Medicine*, vol. 46, no. 6, pp. 983–995, 2005.
- [33] H. Y. Lee, Z. Li, K. Chen et al., “PET/MRI dual-modality tumor imaging using arginine-glycine-aspartic (RGD)-conjugated radiolabeled iron oxide nanoparticles,” *Journal of Nuclear Medicine*, vol. 49, no. 8, pp. 1371–1379, 2008.
- [34] J. S. Choi, J. C. Park, H. Nah et al., “A hybrid nanoparticle probe for dual-modality positron emission tomography and magnetic resonance imaging,” *Angewandte Chemie - International Edition*, vol. 47, no. 33, pp. 6259–6262, 2008.
- [35] J. Xie, K. Chen, J. Huang et al., “PET/NIRF/MRI triple functional iron oxide nanoparticles,” *Biomaterials*, vol. 31, no. 11, pp. 3016–3022, 2010.
- [36] J. H. Maeng, D. H. Lee, K. H. Jung et al., “Multifunctional doxorubicin loaded superparamagnetic iron oxide nanoparticles for chemotherapy and magnetic resonance imaging in liver cancer,” *Biomaterials*, vol. 31, no. 18, pp. 4995–5006, 2010.
- [37] C. Sun, C. Fang, Z. Stephen et al., “Tumor-targeted drug delivery and MRI contrast enhancement by chlorotoxin-conjugated iron oxide nanoparticles,” *Nanomedicine*, vol. 3, no. 4, pp. 495–505, 2008.
- [38] S. Langereis, J. Keupp, J. L. J. Van Velthoven et al., “A temperature-sensitive liposomal 1H CEST and 19F contrast agent for MR image-guided drug delivery,” *Journal of the American Chemical Society*, vol. 131, no. 4, pp. 1380–1381, 2009.
- [39] K. Na, E. S. Lee, and Y. H. Bae, “Adriamycin loaded pullulan acetate/sulfonamide conjugate nanoparticles responding to tumor pH: pH-dependent cell interaction, internalization and cytotoxicity in vitro,” *Journal of Controlled Release*, vol. 87, no. 1–3, pp. 3–13, 2003.
- [40] E. K. Lim, Y. M. Huh, J. Yang, K. Lee, J. S. Suh, and S. Haam, “PH-triggered drug-releasing magnetic nanoparticles for cancer therapy guided by molecular imaging by MRI,” *Advanced Materials*, vol. 23, no. 21, pp. 2436–2442, 2011.
- [41] M. C. Franchini, G. Baldi, D. Bonacchi et al., “Bovine serum albumin-based magnetic nanocarrier for MRI diagnosis and hyperthermic therapy: a potential theranostic approach against cancer,” *Small*, vol. 6, no. 3, pp. 366–370, 2010.
- [42] J. T. Jang, H. Nah, J. H. Lee, S. H. Moon, M. G. Kim, and J. Cheon, “Critical enhancements of MRI contrast and hyperthermic effects by dopant-controlled magnetic nanoparticles,” *Angewandte Chemie - International Edition*, vol. 48, no. 7, pp. 1234–1238, 2009.
- [43] M. K. Yu, Y. Y. Jeong, J. Park et al., “Drug-loaded superparamagnetic iron oxide nanoparticles for combined cancer imaging and therapy in vivo,” *Angewandte Chemie - International Edition*, vol. 47, no. 29, pp. 5362–5365, 2008.
- [44] K. Park, S. Lee, E. Kang, K. Kim, K. Choi, and I. C. Kwon, “New generation of multifunctional nanoparticles for cancer imaging and therapy,” *Advanced Functional Materials*, vol. 19, no. 10, pp. 1553–1566, 2009.
- [45] C. G. Hadjipanayis, M. J. Bonder, S. Balakrishnan, X. Wang, H. Mao, and G. C. Hadjipanayis, “Metallic iron nanoparticles for MRI contrast enhancement and local hyperthermia,” *Small*, vol. 4, no. 11, pp. 1925–1929, 2008.
- [46] B. Chertok, B. A. Moffat, A. E. David et al., “Iron oxide nanoparticles as a drug delivery vehicle for MRI monitored magnetic targeting of brain tumors,” *Biomaterials*, vol. 29, no. 4, pp. 487–496, 2008.
- [47] M. Mahmoudi, A. Simchi, M. Imani, and U. O. Hafeli, “Superparamagnetic iron oxide nanoparticles with rigid cross-linked polyethylene glycol fumarate coating for application in imaging and drug delivery,” *Journal of Physical Chemistry C*, vol. 113, no. 19, pp. 8124–8131, 2009.
- [48] G. Liu, Z. Wang, J. Lu et al., “Low molecular weight alkyl-polycation wrapped magnetite nanoparticle clusters as MRI probes for stem cell labeling and in vivo imaging,” *Biomaterials*, vol. 32, no. 2, pp. 528–537, 2011.
- [49] J. K. Hsiao, C. P. Tsai, T. H. Chung et al., “Mesoporous silica nanoparticles as a delivery system of gadolinium for effective human stem cell tracking,” *Small*, vol. 4, no. 9, pp. 1445–1452, 2008.
- [50] Y. Song, X. Xu, K. W. MacRenaris, X. Q. Zhang, C. A. Mirkin, and T. J. Meade, “Multimodal gadolinium-enriched DNA-gold nanoparticle conjugates for cellular imaging,” *Angewandte Chemie - International Edition*, vol. 48, no. 48, pp. 9143–9147, 2009.

